Article:
Hussain, S, Jamwal, PK, Ghayesh, MH et al. (2017) Assist-as-Needed Control of an Intrinsically Compliant Robotic Gait Training Orthosis. IEEE Transactions on Industrial Electronics, 64 (2). pp. 1675-1685. ISSN: 0278-0046

https://doi.org/10.1109/TIE.2016.2580123

Assist-as-Needed Control of an Intrinsically Compliant Robotic Gait Training Orthosis

Shahid Hussain, Prashant K. Jamwal, *Member*, *IEEE,* Mergen H. Ghayesh, and Sheng Q. Xie, *Senior Member, IEEE*

***Abstract*— It is a common hypothesis in the field of robot assisted gait rehabilitation that the active involvement and voluntary participation of neurologically impaired subjects in the robotic gait training process may enhance the outcomes of such therapy. An adaptive seamless assist-as-needed (AAN) control scheme was developed for the robotic gait training. The AAN control scheme learns in real time the disability level of human subjects based on the trajectory tracking errors and adapts the robotic assistance accordingly. The overall AAN control architecture works on the basis of a robust adaptive control approach. The performance of seamless AAN control scheme was evaluated during treadmill training with a compliant robotic orthosis having 6-degrees of freedom (DOF). Two experiments, namely trajectory following experiment and the AAN experiment were carried out to evaluate the performance of seamless adaptive AAN control scheme. It was found that the robotic orthosis is capable of guiding the subjects' limbs on reference trajectories during the trajectory following experiment. Also, a variation in robotic assistance was recorded during the AAN experiment based on the voluntary participation of human subjects. This work is an advance on the current state of the art in the compliant actuation of robotic gait rehabilitation orthoses in the context of seamless AAN gait training.**

***Index Terms*— Assist-as-needed, compliance adaptation, gait training, pneumatic muscle actuators, intrinsically compliant, robotic orthosis.**

I. INTRODUCTION

REHABILITATION treatment of gait in patients suffering from neurologic impairments [1-3] such as stroke [4-6] and spinal cord injuries (SCI) can be significantly improved with the aid of robotic orthoses [7-9]. Active use of robotic devices during rehabilitation treatments can benefit both, the patient and the therapist significantly. While therapists can get rid of labor intensive and time consuming training sessions, patients can receive objective treatment augmented with the haptic and visual interfaces[10, 11]. The overall rehabilitation process is expected to improve since the use of various sensors and intelligent controller eventually reduce subjectivity by increasing visibility in the recuperation process through data recording and analyses.

Actuation and control technology plays an important role in the design and functioning of these robotic gait training orthoses [12, 13]. The initial prototypes of robotic gait training orthoses were designed using linear actuators such as electric motors which have high endpoint impedance. One of the first gait rehabilitation robots (LOKOMAT), which made use of the body weight support system (BWS) and an automated treadmill, was developed in the late 1990's and after two decades it is still being used in several clinics. LOKOMAT is powered by linear motors [14]. Active Leg Exoskeleton (ALEX) [5] is also powered by linear motors. Ambulation-assisting Robotic Tool for Human Rehabilitation (ARTHUR) [15] makes use of linear motors and a parallel mechanism for gait rehabilitation.

Most of the early gait rehabilitation robots, such as LOKOMAT, make use of trajectory tracking controller [14]. However, such type of controller may not be suitable in carrying out the rehabilitation treatment effectively since it forces patients to follow a fixed trajectory. In fact, for an effective treatment, patients should be encouraged to participate actively and the role of rehabilitation robots should be to only scaffold or support when it is required [8]. Keeping this in view, several control strategies, namely, compliant [9], assist-as-needed (AAN) [5, 16-18] and patient cooperative approaches [9, 19] have been developed in order to regulate robotic assistance with patient's disability levels [12]. A state of the art review of gait rehabilitation robot designs and their control strategies has been provided in [12, 20].

The most common AAN robotic gait training strategies are based on impedance control [21-23]. In order to provide AAN gait training, an impedance control scheme has been implemented on LOKOMAT [24]. An adaptive impedance control scheme has also been proposed in [22]. The impedance controlled robotic devices such as LOKOMAT address the problem of moving compliantly against the gravity by adding an offset term proportional to the weight or a fixed model of the subject's lower extremity dynamics [9, 22]. However, the offset term or fixed model needs to be manually adjusted for

Manuscript received November 3, 2015; revised February 4, 2016, March 9, 2016 and April 13, 2016; accepted April 14, 2016. This work was supported in part by the start-up grant from Faculty of Engineering and Information Sciences, University of Wollongong, NSW, Australia.

S. Hussain is with the School of Mechanical, Materials and Mechatronic Engineering, University of Wollongong, NSW, 2522, Australia (e-mail: shussain@uow.edu.au)

P. K. Jamwal is with the Electrical & Electronics Engineering Department, Nazarbayev University, Astana, 010000, Kazakhstan (e-mail: prashant.jamwal@nu.edu.kz).

M. H. Ghayesh is with the School of Mechanical Engineering, University of Adelaide, Adelaide, SA, 5005, Australia (e-mail: mergen.ghayesh@adelaide.edu.au).

S.Q. Xie is with the Department of Mechanical Engineering, The University of Auckland, Auckland, 2522, New Zealand (e-mail: s.xie@auckland.ac.nz.

each patient [25]. Moreover, the impedance control has only been implemented effectively for the swing phase of robot assisted gait [9, 22]. It is also evident that the lower limb joint stiffness relationship [26, 27] used in the inverse dynamics algorithm of impedance control scheme [9, 22] is most likely not quantitatively identical to that observed in a particular patient.

A force field control scheme [8, 28] has been used by the developers of ALEX [5, 29] and LOKOMAT [17, 30] for the AAN gait training. This control scheme reduces the amount of robotic assistance as the training process progresses in a subjective manner without effectively taking into account the patient's movement capability and disability level. ALEX force field [5] and LOKOMAT impedance controllers (virtual impedance) [24] are also dependent on physical therapist's decision [5, 9]. An AAN control scheme for ALEX has also been evaluated on stroke survivors and has provided encouraging results [31]. Recently, ALEX III is reported in literature and has 12 actively controlled degrees of freedom (DOF) [32]. The adaptive AAN control of ALEX III modulates the assistive force based on the outputs of kernel-based nonlinear filters.

Later, robotic orthoses powered by inherently more compliant actuators have been developed. Pneumatic cylinders have been used by Pelvic Assist Manipulator (PAM) and Pneumatically Operated Gait Orthosis (POGO) [33, 34] to provide compliant actuation to the pelvis and assistance during leg swing. PAM and POGO have used the concept of "triggered assistance" [33]. The triggered assistance encourages the patient to first attempt the movement voluntarily. If the patient fails to perform voluntary movements, then the robotic assistance is provided to complete the movement, either automatically or initiated by a therapist. However, this approach has a discrete-event nature and requires decision either by a programmed rule set or by an observing physical therapist.

Lower Extremity Powered Exoskeleton (LOPES) and Knee-Ankle-Foot Robot (KAFR) [35] are other compliant robotic gait training orthoses. The concept of series elastic actuation (SEA) has been used in the design of LOPES [36] and KAFR. However, the hip joint is not considered in the design of KAFR. The designers of LOPES and KAFR have also considered the concept of AAN gait training [35, 36]. LOPES has its patient-in-charge mode during which the actuator stiffness is kept low and robot-in-charge mode during which the actuator stiffness is set high. A physical therapist's decision is required to manually switch between the patient-in-charge and robot-in-charge mode which does not provide seamless adaptive AAN robotic assistance [36]. A sinusoidal input is used to validate the AAN control of KAFR which is not suitable for gait rehabilitation robots. Also AAN control for KAFR has only been evaluated for ankle joint without the validation for knee joint [35].

Pneumatic muscle actuators (PMA) behave quite similar to the skeletal muscles and therefore these are being used increasingly in the field of rehabilitation robotics [37-40]. PMA have intrinsic elasticity (compliance) which can be used in providing compliant actuation [41]. Several robotic orthoses powered by PMA have been developed for the gait training of neurologically impaired subjects [38, 40, 42-47]. However, in most of the cases, only trajectory-tracking control has been applied to these PMA powered robotic gait training orthoses [38, 48]. Electromyography (EMG) activity of medial gastrocnemius has been used to proportionally control an ankle orthosis powered by PMA [44]. However, the use of EMG signal as a feedback is quite complex [49] and has its own limitations such a cross muscle talk. Hence, the importance of providing seamless, adaptive AAN rehabilitation has been proven to be critical in terms of therapeutic results, at least for the upper limbs [25, 28, 50]. None of the above-mentioned robot control approaches provide such type of gait rehabilitation.

Fig. 1. Experimental setup of the robotic orthosis with a subject walking on a treadmill.

A light weight robotic gait training orthosis powered by PMA had been developed by the authors [48] and subsequently, basic trajectory tracking [51, 52] and adaptive impedance control schemes [22] were implemented and tested. However, the trajectory tracking and impedance control schemes have their own limitations as discussed above. In the present work, we have developed AAN control architecture for providing seamless adaptive robotic assistance during gait training process. The AAN controller adapts the robotic assistance according to the patient's disability level in a seamless manner in real time. The overall AAN control architecture consists of a robust adaptive controller. The basic position controller in the overall AAN control architecture works on the basis of a chattering-free robust variable structure control law (CRVC). CRVC was used as a basic position controller in order to deal with the structured uncertainties in the model of PMA [53]. The adaptive controller in the overall AAN control architecture was developed to adapt the robotic assistance according to subjects' disability level.

It is important to mention here that a seamless adaptive AAN control algorithm has also been developed for Pneu-Wrex by *Wolbrecht et al.* in task space for upper limb rehabilitation [25, 50]. Pneu-Wrex is a robotic orthosis for upper limb rehabilitation and is powered by pneumatic cylinders (cylinder-piston arrangement) [25, 50]. The AAN controller developed in the present study was implemented in joint space whereas the AAN control scheme for Pneu-Wrex has been implemented in task space. The adaptive AAN controller used in this study is different from the controller

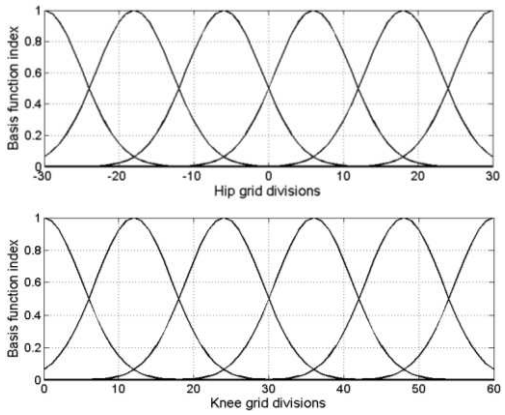

Fig. 2. Radial Basis functions for the hip and knee joints.

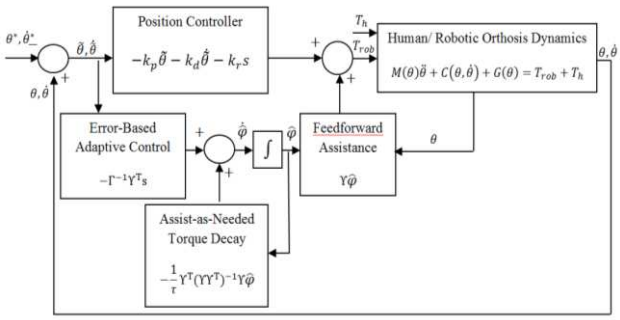

Fig. 3. Overall seamless adaptive Assist-as-Needed (AAN) control architecture. Position controller works on the basis of CRVC control law [51]. The AAN torque decay term continuously decrease the amount of robotic assistance if trajectory tracking errors are small. The AAN controller was implemented in joint space.

used by *Wolbrecht et al*. in a way that a proportional derivative (PD) controller has been used as a basic position controller for Pneu-Wrex [25, 50]; whereas in this study the robust CRVC was used as the basic position controller. It was necessary to use CRVC as the basic position controller because of the structured uncertainties in the model of PMA.

The significance of this work lies in the development of a seamless AAN control scheme for robot assisted gait rehabilitation. This work will help in further developing AAN gait rehabilitation strategies for robotic orthoses powered by intrinsically compliant actuators.

II. METHODOLOGY

A. Robotic Orthosis Design and Modeling

1) Design: A six DOF intrinsically compliant unilateral robotic gait training orthosis powered by pneumatic muscle actuators has been developed for treadmill training of subjects suffering from neurologic impairments (Fig. 1) [48]. The unilateral robotic orthosis presents an effective design choice for the patients with hemiparetic gait. The actuated DOF were hip and knee sagittal plane rotations. All other DOF were kept passive. PMA was used for providing actuation to robotic orthosis hip and knee sagittal plane rotations. The reader is referred to [48] for the complete design description of the robotic gait training orthosis.

2) Modeling: The combined dynamics of robotic orthosis and human subject is given by

$$M(\theta)\ddot{\theta} + C(\theta,\dot{\theta})\dot{\theta} + G(\theta) = T_{rob} + T_h \quad (1)$$

where θ, $\dot{\theta}$, $\ddot{\theta} \in \mathbb{R}$ represent the (hip or knee) angular position, velocity and acceleration, respectively. The dynamics of hip and knee angles have been treated in a decoupled fashion in order to simplify their complex treatment and therefore the overall dynamic equation can be described by (1). Decoupling the hip and knee systems allows us to develop the same controller structure for both subsystems; however the numerical values of their system parameters and their controller gains can be different. $M(\theta) \in \mathbb{R}$ is the inertia term, $C(\theta,\dot{\theta}) \in \mathbb{R}$ represents centrifugal and Coriolis torques, while $G(\theta) \in \mathbb{R}$ includes the gravitational and frictional torques. In the remainder of the paper, the dependence of these terms on θ and $\dot{\theta}$ will be omitted when necessary for the sake of readability. The dependence of variables on time is also omitted for the same reason. The control variable $T_{rob} \in \mathbb{R}$ is the torque applied by the robotic orthosis to the dynamics of hip or knee joint, and is measured by the pressure transducer in the orthosis actuators. Finally, $T_h \in \mathbb{R}$ is the equivalent torque provided by the human subject's leg at the hip joint or knee joint. The passive DOFs of the robotic orthosis also contribute torques at the actuated DOFs. However, these torques were ignored while modeling the actuated DOFs of the robotic orthosis. This assumption was made in order to keep the dynamics of the system simple for control purpose.

Modeling of the robotic orthosis powered by PMA was a crucial task. We refer the reader to [51] for further details regarding the development of the robotic orthosis model, powered by PMA.

B. Assist-as-Needed Control Law

The adaptive controller for the robotic gait training orthosis was implemented in joint space for the hip and knee sagittal plane rotations. Each of the two adaptive controllers makes use of the sliding variable s and of the "reference trajectory" v [25, 50, 54]. Here, s and v are defined as

$$s = \dot{\tilde{\theta}} + \lambda\tilde{\theta} \quad (2)$$

$$v = \dot{\theta}^* - \lambda\tilde{\theta} \quad (3)$$

where $\tilde{\theta} = \theta - \theta^*$ describes each of the tracking errors (at hip and knee joints), θ^* and θ being the desired and actual joint angles, respectively. Also, $\lambda = 4\,Hz$ is a design parameter, which was chosen experimentally. It was assumed that the joint angles of the robotic orthosis correspond to the joint angles of the human subject. Numerical differentiation was used to calculate joint angular velocities. A single-rate differentiator filter with an order of 31 and a cutoff frequency of 200 Hz was implemented using Matlab to perform the smoothening operation.

As a first step towards the definition of the control law, following the development in [25], we define the term

$$Y(\theta,\dot{\theta},v,\dot{v})\varphi = M\dot{v} + Cv + G - T_h \quad (4)$$

which represents the dynamics of θ and v, in which $\varphi \in \mathbb{R}^6$ is a column vector of parameters (representing the amount of torque the subject is unable to provide to complete the desired joint motions), while $Y(\theta,\dot{\theta},v,\dot{v}) \in \mathbb{R}^{1\times 6}$ is a row vector of basis functions, assumed known, whose dependence on its arguments will be also omitted in the subsequent development of the paper. Since we assume that the time-varying functions M, C, G and T_h are unknown, we define the term

$$Y\hat{\varphi} = \hat{M}\dot{v} + \hat{C}v + \hat{G} - \hat{T}_h \quad (5)$$

analogous to (4), where each term with superscript represents the current estimate of the corresponding unknown term (e.g., $\widehat{M}$ is the estimate of M). In particular, $\hat{\varphi} \in \mathbb{R}^6$ is the vector of estimates of the actual system parametersφ. The term $Y\hat{\varphi}$ will be a first component of the overall control law. Conventionally, classical dynamic modeling methods have been used to develop the dynamic model in (5). This latter, which includes the human joint torque component (T_h), should have sufficient resolution to adapt to different types and levels of neurologic impairments. The dynamic model developed for the robotic gait training orthosis in this study used a Gaussian radial basis function to model the human joint torque component, as in [25]. The Gaussian radial basis functions for each of the two angles are defined as

$$g_i = \exp\left(-\frac{|\theta-\mu_i|}{2\sigma^2}\right) \quad (7)$$

where μ_i is the center of the *i-th* radial basis function, θ is the current value of the subject's joint angle and σ is a scalar smoothing constant that determines the width of the basis function. The grid divisions (Fig. 2) were equally spaced at 12^o apart with $\sigma = 5.096^o$for both subsystems. The number of basis functions and the value of σ were chosen experimentally, in order to offer the best possible trade-off between the precision of the approximation, and the computational complexity of the implemented controller. The vector of all the Gaussian radial basis functions is defined as

$$Y = [g_1 \quad g_2 \quad g_3 \quad g_4 \quad g_5 \quad g_6]^T \quad (6)$$

The parameter vector is updated over time, according to the following dynamics, analogously to what is done in [25]:

$$\dot{\hat{\varphi}} = -\frac{1}{\tau}Y^T(YY^T)^{-1}Y\hat{\varphi} - \Gamma^{-1}Y^T s \quad (7)$$

Recalling the fact that $Y\hat{\varphi}$ is a component of the control law, we can notice that the first term on the RHS of (7) tends to reduce the control action, and decays with time constant $\tau \in \mathbb{R}$. This term is aimed at letting the information learned from the previous motion be preserved in $\hat{\varphi}$, which is very useful in case the human subject repeats a similar motion over time. The second term on the right hand side (RHS) of (7) is instead attempting to reduce the tracking error, and is a typical adaptive control term, in which $\Gamma = \gamma I \in \mathbb{R}^{6\times6}$ determines the overall error- based adaptation rate, with $\gamma = 11N/m$ chosen experimentally. The dynamics in (7) is supposed to enforce a decrease of the torque applied by the robotic gait training orthosis when the subject is able to complete the movements without robotic assistance, which is the main characteristic of AAN schemes.

The overall robust adaptive control law (Fig. 3) for the desired robotic joint torque is written as

$$T_{rob} = Y\left(\theta, \dot{\theta}, v, \dot{v}\right)\hat{\varphi} - k_p\tilde{\theta} - k_d\dot{\tilde{\theta}} - k_r s \quad (8)$$

A CRVC law is used as a basic position controller, to guide the subject's limbs on reference trajectories in the presence of structured uncertainties in the model of PMA. The terms $k_p \in \mathbb{R}$ and $k_d \in \mathbb{R}$ are positive constants, representing proportional and derivative gains, while k_r is a time-varying scalar function which implements the CRCV action, and is implicitly defined by the expression

$$sk_r = \alpha \cdot \text{sign}(s) \cdot (F + D|sk_r|) \quad (9)$$

where , F, $D \in \mathbb{R}$ are positive design parameters. This CRCV term is a simplified version of the robust control action applied in [51]. In the latter paper, the uncertainty was completely compensated by the robust (CRCV) control action, while in the present paper the adaptive term is mainly used to compensate for the uncertainty due to the presence of the human subject, and the CRCV term to compensate for the uncertainty related to the actuator dynamics. By increasing the magnitude of the design parameters α, F and D (which have been determined experimentally), a larger energy is allocated to the CRCV control term, in order to cope with increasing uncertainty in the PMA dynamics.

Lyapunov stability analysis of the robust adaptive AAN control scheme is provided in the APPENDIX. The human torque component in the AAN controller is certainly time-dependent. The presence of a time-dependent human torque component results in an overall control system that is not globally asymptotically stable. However, it can be shown that the proposed controller imposes a closed-loop dynamics for the tracking errors that is ultimately bounded. This means that, after a transient phase, each of the two tracking errors is confined inside a compact set, whose size depends both on the parameters of the system and on the torque output from the human subject (please see APPENDIX).

III. Experimental Evaluation

A. Subjects

Ten healthy, neurologically intact subjects (8 male and 2 female, age 25-42 years (Mean (M) 31.5 years and Standard Deviation (SD) 6.6039), height (M 1.702m and SD 0.056m) and weight (M 69.6Kg and SD 6.391)) with no history of neurologic disorders gave written informed consent and participated in the preliminary study. The University of Auckland, Human Participants Ethics Committee approved this protocol.

B. Experiment Protocol

The subjects were asked to walk within the passive (zero assistance mode) robotic orthosis for 20 minutes so that they should become familiar with the robotic orthosis and training environment. Similar procedure was repeated for the robotic orthosis in trajectory tracking (active) mode. All the experiments were conducted in single session. A wash out period of 20 minutes, for every subject, between each experiment mode was also provided. Hip and knee sagittal plane physiological gait trajectories reported by *Winter* in [55] were used to define the reference joint angle trajectories. These joint angle trajectories are scalable in time, amplitude offset and range in order to be adjusted to the individual gait parameters of subjects. However, this scaling was not performed during the current experiments. Walking speed was set to 0.6 m/s during all experiments. Sensor data for all the experiments was collected at 60 *Hz*. No BWS was used during the experiments as the test subjects had no neurologic impairments and did not require any external support [29, 56]. The following experimental protocol was developed to evaluate the performance of AAN control scheme.

1) Trajectory Following Experiment: Trajectory following experiment is divided into two modes. During the first mode the subjects were asked to track the reference joint angle trajectories in a passive robotic orthosis (*zero assistance mode*). During the zero assistance mode the robotic orthosis

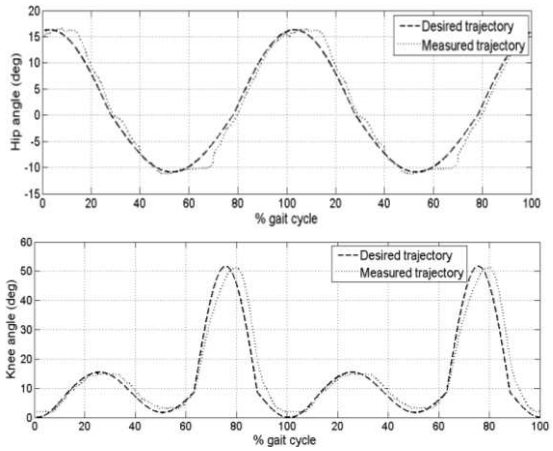

Fig. 4. Average hip and knee sagittal plane joint angle trajectories with healthy subjects as a percentage of gait cycle (GC) obtained during position control mode (trajectory tracking), averaged over all subjects for two GC. The shown trajectories are for the values of forgetting rate ($\tau = 8$s) that still allows the robotic orthosis to move the subjects' limbs on reference trajectories.

was operated in the *zero impedance* or *zero force* mode. The terms of *backdrive* [25], *patient-in-charge* [36] and *zero impedance control* [9] have also been used for this zero assistance mode in literature. In this mode the robotic gait training orthosis balanced its own weight and the net torque at the joint level was zero. Visual feedback was used to show the subjects their tracking performance and encourage them to track the reference trajectories. A computer monitor was used to provide the graphical display of the reference joint angle trajectories to the subjects along with their achieved trajectories in real time. After the initial 20 minute session the data for 60 gait cycles (GC) during the zero assistance mode was recorded for analysis purpose. The rationale for the initial 20 minute session was that to familiarize the subjects with the robotic orthosis walking. During the second mode (*position control mode*) the subjects were instructed to remain passive within the robotic orthosis and allow it to guide the trajectory of their legs during the AAN control mode. Data for 60 GC was recorded during position control mode for analysis purpose. The forgetting rate τ for the AAN controller was chosen by trial and error during the experiments. The value of τ was slowly decreased until the controller could no longer move the subjects' limbs on reference trajectories. A maximum trajectory tracking error of 10^o was used during the determination of value of τ. If the trajectory tracking error goes beyond 10^o, it was assumed that the controller is no longer able to move the subject's limbs on reference trajectories. This position control mode is important for the gait training of severely impaired subjects who cannot voluntarily participate towards the gait training process. Visual feedback was not used during the position control mode. The value of forgetting rate, $\tau = 8s$ or $(1/\tau = 0.125)$ that can still guide the subject's limbs on reference trajectories was used for subsequent AAN experiments.

2) AAN Experiment: One more experiment was designed to evaluate if the AAN control scheme could learn the torques necessary to assist the subjects in achieving the desired ranges of motion while allowing the subject to remain as actively involved in the motions as possible. For the Mode I (*always active mode*) visual feedback was used and the subjects were

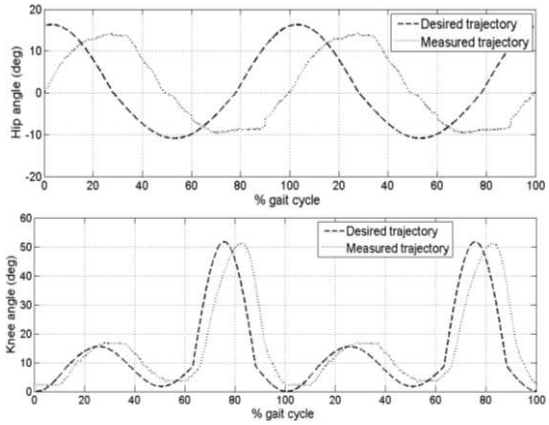

Fig. 5. Average hip and knee sagittal plane joint angle trajectories with healthy subjects as a percentage of GC obtained during zero-impedance control mode, averaged over all subjects for two GC.

TABLE I
MAXIMUM ABSOLUTE VALUES OF SAGITTAL PLANE JOINT ANGULAR DEVIATIONS AND MEAN VALUES OF THE ROBOT COMMANDED JOINT TORQUE FOR DIFFERENT CONTROL MODES AND AVERAGED OVER SUBJECTS DURING TRAJECTORY FOLLOWING EXPERIMENT. THE JOINT TORQUE IS A ROUGH INDICATOR OF THE ROBOTIC ASSISTANCE PROVIDED TO THE SUBJECTS. STANDARD DEVIATIONS (±) ARE PRESENTED FOR INTER-SUBJECT VARIABILITY.

Gait parameter	Zero assistance mode	Position control mode	
		$\tau = \infty$	$\tau = 8s$
$\lvert\tilde{\theta}_{hip}\rvert_{\max}$	$18.78^o \pm 7.5$	$2.96^o \pm 1.7$	$4.22^o \pm 2.1$
$\lvert\tilde{\theta}_{knee}\rvert_{\max}$	$28.24^o \pm 10.2$	$6.31^o \pm 2.05$	$7.1^o \pm 2.5$
$\lvert T_{rob,hip}\rvert$	0	33.1 Nm±2.2	26.3 Nm±1.8
$\lvert T_{rob,knee}\rvert$	0	31.21 Nm±1.9	21.1 Nm±1.6

asked to track the reference joint angle trajectories for 60 GC. The objective of always active mode was to see if the AAN control scheme can learn the torques necessary to assist the subjects in tracking the joint angle trajectories while allowing the subjects to be more actively involved in the gait training process.

For the Mode II (*inactive to active mode*) the subjects were instructed to remain passive within the robotic orthosis and allow it to guide the trajectory of their legs during the first 20 GC. During these 20 GC the controller learned the model of the torques necessary to guide the subject's limbs on reference trajectories. After the first 20 GC the subjects were asked to actively track the joint angle trajectories while using visual feedback for 40 GC. The aim of inactive to active mode was to determine if the AAN controller can reduce its torque output (T_{rob}) to allow increased voluntary output from the subjects. Both the always active and inactive to active modes were evaluated with no forgetting rate ($\tau = \infty$) and a forgetting rate ($\tau = 8s$) included in the AAN controller to evaluate the effect of forgetting rate.

The experiments were performed in the following order for all the subjects. Firstly, the trajectory following experiment was performed. Zero assistance mode was performed prior to the position control mode. Secondly, AAN experiment was performed. Always active mode was performed prior to the inactive to active mode.

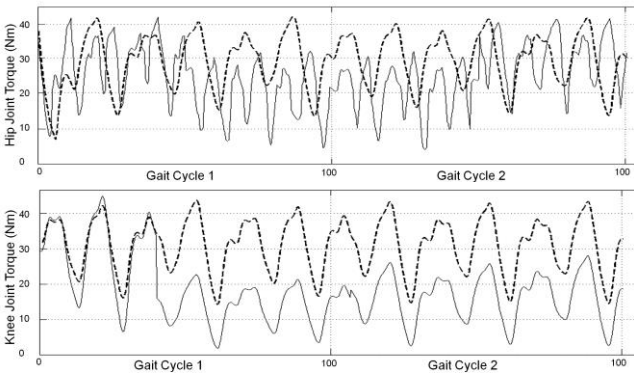

Fig. 6. Robotic orhtosis commanded torques at hip and knee sagittal plane joints of healthy subjects as a percentage of GC obtained during AAN experiment for always active condition, averaged over all subjects for two GC. Trajectories with a forgetting term ($\tau = 8s$) (solid line) and without a forgetting term ($\tau = \infty$) are shown (dotted line)

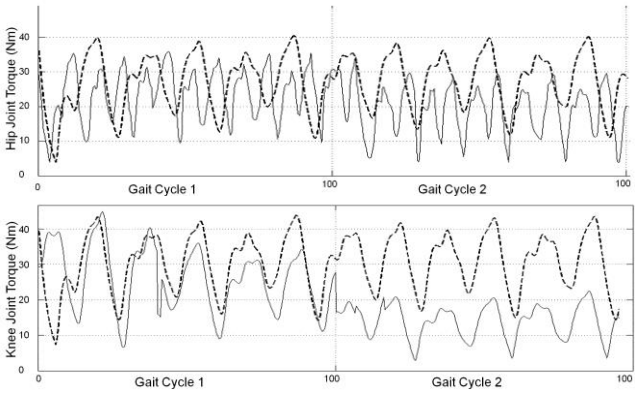

Fig. 7. Robotic orthosis commanded torques at hip and knee sagittal plane joints of healthy subjects as a percentage of GC obtained during AAN experiment for inactive to active condition, averaged over all subjects for two GC. Trajectories with a forgetting term ($\tau = 8s$) (solid line) and without a forgetting term ($\tau = \infty$) are shown (dotted line). The subjects' remained inactive (passive) during GC1. At the end of GC1 the subjects' participated actively in the gait training process during GC2.

TABLE II

MAXIMUM ABSOLUTE VALUES OF SAGITTAL PLANE JOINT ANGULAR DEVIATIONS AND MAXIMUM VALUE OF THE CONTROLLER OUTPUT (I.E. ROBOT COMMANDED) JOINT TORQUES FOR DIFFERENT CONTROL MODES AND AVERAGED OVER SUBJECTS DURING ASSIST-AS-NEEDED EXPERIMENT. THE JOINT TORQUE IS THE ROUGH INDICATOR OF THE ROBOTIC ASSISTANCE PROVIDED TO THE SUBJECTS. STANDARD DEVIATIONS (±) ARE PRESENTED FOR INTER-SUBJECT VARIABILITY AND P-VALUES FROM WILCOXON SIGNED-RANK TEST FOR BOTH MODES ARE ALSO PROVIDED. VALUES FOR GC2 PRESRENTED IN FIG. 6 AND FIG. 7 ARE PROVIDED.

Gait parameter	Mode I (Always active)		Mode II (Inactive to active)		*P*-values	*P*-values
	$\tau = \infty$	$\tau = 8s$	$\tau = \infty$	$\tau = 8s$	$\tau = \infty$ (Modes I&II)	$\tau = 8s$ (Modes I&II)
$\lvert\tilde{\theta}_{hip}\rvert_{\max}$	3.16°±2.4	6.52°±1.82	4.62°±3.71	6.13±2.9	0.0020	0.1309
$\lvert\tilde{\theta}_{knee}\rvert_{\max}$	5.22°±3.52	6.5°±1.73	5.84°±2.3	6.95±2.8	0.0039	0.9219
$\lvert T_{rob,hip}\rvert_{\max}$	42.3 Nm±3.1	38.1 Nm±2.6	42.6 Nm±2.7	35.5 Nm±3.2	0.0045	0.0020
$\lvert T_{rob,knee}\rvert_{\max}$	46.51 Nm±2.4	27.1 Nm±3.2	44.5 Nm±3.7	28.2 Nm±4.6	0.0020	0.0016

C. Data Analysis

Intra-subject variability is an important parameter to study the reproducibility of the experimental results. In order to study the intra-subject variability, standard deviations of the sagittal plane maximum joint angular deviations ($\lvert\tilde{\theta}_{hip}\rvert_{\max}$, $\lvert\tilde{\theta}_{knee}\rvert_{\max}$) and sagittal plane robotic joint torques values $\lvert T_{rob}\rvert$ from different GC of each separate experimental mode were assessed. Further, in order to evaluate the statistical significance of the experimental outcomes a Wilcoxon signed-rank test [57] was also performed and discussed. All the statistical tests were performed using MATLAB R2009b (The MathWorks, Inc: Natick, Ma, USA).

IV. EXPERIMENTAL RESULTS

A. Trajectory Following Experiment

The desired and measured hip and knee sagittal plane joint angle trajectories during position control mode are shown in Fig. 4. The presented results (Fig. 4) are for the minimum value of forgetting rate ($\tau = 8s$) that can still provide sufficient robotic assistance to guide the subject's limbs on reference trajectories. This minimum value of the forgetting rate was also used in the AAN experiments. The trajectories (Fig. 4) were averaged over all subjects for two GC. The angular deviations ($\lvert\tilde{\theta}_{hip}\rvert_{\max}$, $\lvert\tilde{\theta}_{knee}\rvert_{\max}$) form the reference joint angle trajectories averaged over all subjects are provided in Table I (mean of maximum errors is provided). During position control mode the maximum allowable angular deviations from desired hip and knee joint angle trajectories were below 10° (maximum mean values depicted in Table I). The mean values of robot commanded torque ($\lvert T_{rob}\rvert$) averaged over all subjects during position control mode are presented in Table I. With an inclusion of the forgetting term, a decrease in robotic assistance was observed for all subjects as compared to the condition during which the forgetting term was not included ($\tau = \infty$) (values depicted in Table I). The desired and measured hip and knee joint angle trajectories during the zero assistance mode, averaged over all subjects for two GC are shown in Fig. 5. The magnitude of angular deviations (trajectory-tracking errors) during the zero assistance mode were 18.78° and 28.24° for hip and knee joints, respectively, which were higher as compared to the position control mode values of 4.22° and 7.1° for hip and knee joints, respectively (values depicted in Table I). This shows that the subject had the freedom to perform voluntary movement during the zero assistance mode. The commanded torque of the robotic orthosis at the joint level was zero during the zero assistance mode (Table I)

B. AAN Experiment

The AAN experiment was also performed for two modes. During the always active mode the subjects were actively participating in the gait training process. The second condition

of inactive to active mode was evaluated to see that whether the robotic orthosis can reduce the applied joint torques if the subjects are actively participating in the gait training process. For the AAN experiment the maximum joint angle deviations from the reference trajectories were also kept below 10^o by the robotic orthosis.

The robotic orthosis joint torques (T_{rob}) during the always active mode and inactive to active mode are shown in Fig. 6 and 7, respectively. With an inclusion of the forgetting term in the AAN controller, the robotic assistance (T_{rob}) decreased to 38.1 Nm and 27.1 Nm at hip and knee joint, respectively during the always active mode (Fig. 6), whereas without a forgetting term the robotic orthosis applied higher joint torques of about 42.3 Nm and 46.51 Nm at hip and knee joint, respectively, despite the fact that the subjects' were actively contributing in the gait training process. The magnitude of maximum values of these robot commanded joint torques averaged over all subjects are provided in Table II.

In order to show that the robotic assistance decreases during AAN gait training, the robot torques (T_{rob}) during the inactive to active mode averaged over all subjects is presented for two GC (Fig. 7). During the GC1 the subjects were inactive and were not voluntarily participating in the robotic gait training process. During the GC2 the subjects were actively contributing in order to achieve the desired trajectories (Fig. 7). When the forgetting term ($\tau = 8s$) was included in the AAN controller, the robot commanded torques decreases from 42.6 Nm to 35.5 Nm and 44.5 Nm to 28.2 Nm for hip and knee joints, respectively as the subjects' started to participate in the robotic training process (Fig. 7 and Table II). Without a forgetting term ($\tau = \infty$) the robot commanded torques did not show a decreasing trend during the inactive to active mode. In other words the robotic orthosis commanded torque during the inactive to active mode without a forgetting term (Fig. 7) showed a similar pattern as observed in the always active mode without a forgetting term (Fig. 6). This shows that without the forgetting term the robotic orthosis did not decrease the assistance torque (T_{rob}) during the AAN experiment and hence resulted in a reduction of the voluntary participation from the human subjects. The robotic assistance during the inactive to active mode (Fig. 7) converged to a steady state value depending upon the value of forgetting rate and the amount of voluntary participation from the human subjects.

With an inclusion of forgetting term, a decrease in robotic assistance was observed for all subjects as compared to the condition during which the forgetting term was not included ($\tau = \infty$) (values depicted in Table II). The maximum mean values of trajectory tracking errors averaged over all subjects during the always active mode and inactive to active mode are presented in Table II (error values of only GC 2 are provided).

It was ensured during the AAN experiments that the deviations from reference joint angle trajectories must be below 10^o. These angular deviations are partly due to the structured uncertainties in the model of PMA [53]. If the trajectory tracking errors go beyond 10^o, the robotic orthosis should enhance its assistance torque. The subjects felt comfortable during all the experiments and no complaints of pain were reported. The passive foot lifter provided sufficient dorsiflexion during the swing phase and no cases of foot touching the treadmill were observed during the experiments.

Finally, in order to check whether the differences in observations from two modes of AAN experiments (always active mode and inactive to active mode) are statistically significant, a Wilcoxon signed-rank test was performed. The null hypothesis being tested was that there is no statistically significant difference between observations across the two modes of experiment. It should be emphasized that a nonparametric approach was exploited as the data sample size was small. Significance threshold 0.01 was considered to evaluate the statistical significance. Therefore, p-values less than 0.01 indicate the null hypothesis being rejected. In our study, this threshold is almost equivalent to the usual threshold of 0.05 adjusted with the Bonferroni multiple hypothesis test correction for our experimental protocols having four test parameters ($0.05/4 = 0.0125$). Results of the signed-rank test are presented in Table II. It is evident from the results that for most of the observations, the null hypothesis can be rejected owing to the small p-values. However, at least two observations (maximum absolute values of joint angular deviations during $\tau = 8s$) failed to reject the null hypothesis ($p > 0.01$). This further means that although a change in the angular deviation is observed when the forgetting factor was included, it is not statistically significant. This may be, primarily, due to the fact that the provisions in the controller do not allow deviations from reference joint angle trajectories beyond a threshold value. Nevertheless, there is noticeable change in the commanded torques, which further strengthens the presumption that inclusion of forgetting factor enhances controller's ability to provide customized assistance by varying the commanded torques. Further, observations from Table II, (mode II) reveal that including forgetting factor into the controller ($\tau = 8s$), the angular deviations increases whereas the commanded torques decreases significantly. This is an important inference which further means that by reducing the commanded torque, controller allowed increased voluntary output from the subjects.

V. Discussion And Conclusion

In this work an AAN controller was developed for the robot assisted gait training of neurologically impaired subjects. The overall AAN control architecture works on the basis of a robust adaptive control approach. The overall AAN control architecture uses a robust CRVC law as the basic position controller in order to provide reasonable trajectory tracking performance in the presence of structured uncertainties in the model of PMA. The AAN controller was designed to provide seamless adaptive robotic assistance according to the disability level and stage of rehabilitation of neurologically impaired subjects. We believe that this kind of adaptive AAN robotic gait training is important for neurologically impaired subjects in order to maximize the therapeutic efficacy.

During position control mode the maximum angular deviations from desired hip and knee joint angle trajectories must be below 10^o. This performance is in accordance with the other gait rehabilitation orthoses such as LOKOMAT, for which the maximum trajectory tracking errors during the position control mode must be below 15^o [9]. The position

control mode is important for the severely impaired subjects who are not capable of voluntarily participating in the gait training process during the early phases of rehabilitation. During the zero assistance mode the angular deviations were higher as compared to the position control mode. This phenomenon was observed because the robotic orthosis was completely passive during the zero assistance mode and the subjects have the freedom to drive the robotic orthosis freely. This phenomenon has also been reported for the zero assistance mode of LOKOMAT [9]. The AAN controller takes input in the form of trajectory tracking error and adjusts the robotic assistance. The model based component of the controller adapts in real time the robotic assistance depending on the trajectory tracking errors. If tracking errors are small the controller decays the robotic assistance and lets the subjects complete the desired movements and vice versa. It was observed during the AAN experiment that the inclusion of forgetting factor in the adaptive AAN control scheme resulted in a variation in robot commanded joint torques, depending on the subjects' voluntary participation. When the forgetting rate was not included in the adaptive AAN control scheme, the robotic orthosis did not decay the commanded torques even when the subjects were actively contributing towards the gait training process.

The AAN controller developed in this study is proven theoretically stable by using a Lyapunov-based stability analysis. The AAN controller implemented for the robotic gait training orthosis has the human torque component which is certainly time dependent. The presence of time dependent human torque component results in a system which is not globally asymptotically stable. However, the controller was shown to exhibit ultimate boundedness, with the tracking errors limited by the bounds of the system dynamics and by the bounds of the torque output from the human subject. It was found experimentally that the control law (8) determines a convergence to steady state tracking errors.

The value of forgetting rate was kept same for all the healthy subjects during the experimental evaluation and it provided satisfactory results. However, it will be interesting to see the effect of variation of the forgetting rate on the patients' with different level of disability.

Statistical analysis of the observed data using the Wilcoxon signed-rank test shows that for most of the test data, the null hypothesis was rejected and statistically significant difference was found between observations across the two modes of experiments. However, observations for angular deviations during ($\tau = 8s$) failed to reject the null hypothesis indicating that, though a change can be noticed in the angular deviations, it is not statistically significant. As stated earlier, primarily this may be due to the fact that the controller does not allow angular deviations beyond a threshold value. However, there are other factors which may cause this anomaly, such as, small sample size, involuntary participation of subjects and absence of a body weight support system to neutralize subjects' weights.

In summary, this research presents a seamless adaptive AAN control scheme for the robot assisted gait training of neurologically impaired subjects. The presented control scheme for seamless adaptive AAN gait training was only evaluated on healthy subjects. In order to establish the therapeutic efficacy of the adaptive AAN gait training strategy, rigorous clinical trials with neurologically impaired subjects are necessary. This work will aid in further developing adaptive AAN rehabilitation strategies for robotic systems powered by intrinsically compliant actuators.

APPENDIX

This section describes the Lyapunov stability analysis of the proposed robust adaptive AAN control scheme, mainly based on the results on adaptive algorithms in [25[54]. We formulate only one proof, which can be applied to the dynamics of both hip and knee angles. The Lyapunov function candidate taken into account is

$$V = \frac{1}{2}Ms^2 + \frac{1}{2}(k_p + \lambda k_d)\tilde{\theta}^2 + \frac{1}{2}\tilde{\varphi}^T\Gamma\tilde{\varphi} \tag{10}$$

where $\tilde{\varphi} = \hat{\varphi} - \varphi$ is the time-varying estimation error of the parameter. Differentiating (10) yields

$$\dot{V} = sM\dot{s} + \frac{1}{2}\dot{M}s^2 + (k_p + \lambda k_d)\tilde{\theta}\dot{\tilde{\theta}} + \tilde{\varphi}^T\Gamma\dot{\tilde{\varphi}} \tag{11}$$

By taking the term $M\dot{s} + Cs + Y\varphi$ and substituting the expressions of s, $\dot{s}$, and $Y\varphi$ from (2)-(4), one can show that $M\dot{s} + Cs + Y\varphi = M\ddot{\theta} + C\dot{\theta} + G - T_h$. As a consequence, by simply taking the system dynamics (1) into account,

$$M\dot{s} = T_{rob} - Cs - Y\varphi \tag{12}$$

By using (12), one can further expand the expression of $\dot{V}$ in (11) as

$$\dot{V} = s(T_{rob} - Cs - Y\varphi) + \frac{1}{2}\dot{M}s^2 + (k_p + \lambda k_d)\tilde{\theta}\dot{\tilde{\theta}} + \tilde{\varphi}^T\Gamma\dot{\tilde{\varphi}} \tag{13}$$

Also, since $\tilde{\varphi} = \hat{\varphi} - \varphi$, recalling that (being φ constant over time) $\dot{\varphi} = 0$, and remembering that, by physical properties of the system, $\dot{M} - 2C = 0$, from (13) it is possible to obtain

$$\dot{V} = s(T_{rob} - Y\hat{\varphi}) + (k_p + \lambda k_d)\tilde{\theta}\dot{\tilde{\theta}} + \tilde{\varphi}^T(\Gamma\dot{\hat{\varphi}} + Y^T s) \tag{14}$$

Substituting the expressions of $Y\hat{\varphi}$ in (5), $\dot{\hat{\varphi}}$ in (7), and T_{rob} in (8), yields

$$\dot{V} = -\lambda k_p\tilde{\theta}^2 - k_d\dot{\tilde{\theta}}^2 - k_r s^2 - \tilde{\varphi}^T\Lambda\hat{\varphi} \tag{15}$$

where $\Lambda = \frac{1}{\tau}\Gamma Y^T(YY^T)^{-1}Y \in \mathbb{R}^{6\times 6}$. From (9), it is immediate to obtain that k_r, although time-varying, is always positive. As a consequence

$$\dot{V} \leq -\lambda k_p\tilde{\theta}^2 - k_d\dot{\tilde{\theta}}^2 - \tilde{\varphi}^T\Lambda\hat{\varphi} \tag{16}$$

It is not possible to prove the negative definiteness of $\dot{V}$, since the sign of $\tilde{\varphi}^T\Lambda\hat{\varphi}$ can be either positive or negative. However, one can define $e = [\tilde{\theta} \quad \dot{\tilde{\theta}}]^T \in \mathbb{R}^2$ and $P = \mathrm{diag}(\lambda k_p, k_d) \in \mathbb{R}^{2\times 2}$ and rewrite (16) as

$$\dot{V} \leq -e^T Pe - \tilde{\varphi}^T\Lambda\hat{\varphi} \tag{17}$$

If $e^T Pe > -\tilde{\varphi}^T\Lambda\hat{\varphi}$, then $\dot{V} < 0$. A sufficient condition for this to happen is

$$\lambda_{\min}(P)\|e\|^2 > \max_{\hat{\varphi}}(-\tilde{\varphi}^T\Lambda\hat{\varphi}) \tag{18}$$

where $\lambda_{\min}(P) = \min(\lambda k_p, k_d)$ is the minimum eigenvalue of P. The maximum of $-\tilde{\varphi}^T\Lambda\hat{\varphi}$ occurs when $\hat{\varphi} = \varphi/2$, which implies $\tilde{\varphi} = \varphi/2$. Hence, sufficient condition for $\dot{V} < 0$ is

$$\|e\| > \frac{1}{2}\left(\frac{\varphi^T\Lambda\varphi}{\lambda_{min}(P)}\right)^{1/2} \tag{19}$$

Equation (19) represents the set of the plane, which has $\tilde{\theta}$ and $\dot{\tilde{\theta}}$ as coordinates, in which we can prove that the Lyapunov function is decreasing over time. This means that e converges to the Euclidean ball that is the complement of the set described in equation (19). It is therefore possible to conclude that $\tilde{\theta}$ converges to the set defined as

$$\left|\tilde{\theta}\right| \leq \frac{1}{2}\left(\frac{\varphi^T \Lambda \varphi}{\lambda_{\min}(P)}\right)^{1/2} \quad (20)$$

Recalling the expression of Λ, defined after equation (15), and the fact that $\lambda_{\max}(\Gamma Y^T (Y Y^T)^{-1} Y) = \lambda_{\max}(\Gamma)$, we conclude that $\tilde{\theta}$ is ultimately bounded as follows:

$$\left|\tilde{\theta}\right| \leq \frac{1}{2}\|\varphi\|\left(\frac{1}{\tau}\frac{\lambda_{\max}(\Gamma)}{\lambda_{\min}(P)}\right)^{1/2} \quad (21)$$

This shows that the upper bound on the tracking error after the transient phase is proportional to the Euclidean norm of the actual parameter vector φ of the system (a maximum parameter error of 20% in the model of PMA was selected while formulating the overall control law). Also, the bound is proportional to the forgetting rate $1/\tau$ of the adaptive part of the controller.

REFERENCES

[1] C. M. Dean, C. L. Richards, and F. Malouin, "Walking speed over 10 metres overestimates locomotor capacity after stroke," *Clinical Rehabilitation,* vol. 15, pp. 415-421, Aug. 2001.

[2] H. P. Von Schroeder, R. D. Coutts, P. D. Lyden, E. Billings Jr, and V. L. Nickel, "Gait parameters following stroke: A practical assessment," *Journal of Rehabilitation Research and Development,* vol. 32, pp. 25-31, Feb. 1995.

[3] S. J. Olney, M. P. Griffin, T. N. Monga, and I. D. McBride, "Work and power in gait of stroke patients," *Archives of Physical Medicine and Rehabilitation,* vol. 72, pp. 309-314, Apr. 1991.

[4] B. Husemann, F. Müller, C. Krewer, S. Heller, and E. Koenig, "Effects of locomotion training with assistance of a robot-driven gait orthosis in hemiparetic patients after stroke: A randomized controlled pilot study," *Stroke,* vol. 38, pp. 349-354, Feb. 2007.

[5] S. K. Banala, S. H. Kim, S. K. Agrawal, and J. P. Scholz, "Robot assisted gait training with active leg exoskeleton (ALEX)," *IEEE Transactions on Neural Systems and Rehabilitation Engineering,* vol. 17, pp. 2-8, Feb. 2009.

[6] J. S. Sulzer, R. A. Roiz, M. A. Peshkin, and J. L. Patton, "A highly backdrivable, lightweight knee actuator for investigating gait in stroke," *IEEE Transactions on Robotics,* vol. 25, pp. 539-548, Jun. 2009.

[7] S. Jezernik, R. Schärer, G. Colombo, and M. Morari, "Adaptive robotic rehabilitation of locomotion: A clinical study in spinally injured individuals," *Spinal Cord,* vol. 41, pp. 657-666, 2003.

[8] L. L. Cai, A. J. Fong, C. K. Otoshi, Y. Liang, J. W. Burdick, R. R. Roy*, et al.*, "Implications of assist-as-needed robotic step training after a complete spinal cord injury on intrinsic strategies of motor learning," *Journal of NeuroScience,* vol. 26, pp. 10564-10568, Oct. 2006.

[9] R. Riener, L. Lunenburger, S. Jezernik, M. Anderschitz, G. Colombo, and V. Dietz, "Patient-cooperative strategies for robot-aided treadmill training: First experimental results," *IEEE Transactions on Neural Systems and Rehabilitation Engineering,* vol. 13, pp. 380-394, Sep. 2005.

[10] R. Lu, Z. Li, C. Y. Su, and A. Xue, "Development and learning control of a human limb with a rehabilitation exoskeleton," *IEEE Trans. Ind. Electron.,* vol. 61, pp. 3776-3785, Jul. 2014.

[11] S. Hussain, S. Q. Xie, and P. K. Jamwal, "Effect of Cadence Regulation on Muscle Activation Patterns during Robot Assisted Gait: A Dynamic Simulation Study," *IEEE Journal of Biomedical and Health Informatics* vol. 17, pp. 442-451, Mar. 2013

[12] S. Hussain, S. Q. Xie, and G. Liu, "Robot assisted treadmill training: Mechanisms and training strategies," *Medical Engineering & Physics,* vol. 33, pp. 527-533, Jun. 2011.

[13] J. F. Veneman, R. Ekkelenkamp, R. Kruidhof, F. C. T. Van Der Helm, and H. Van Der Kooij, "A series elastic- and bowden-cable-based actuation system for use as torque actuator in exoskeleton-type robots," *International Journal of Robotics Research,* vol. 25, pp. 261-281, Mar. 2006.

[14] G. Colombo, M. Joerg, R. Schreier, and V. Dietz, "Treadmill training of paraplegic patients using a robotic orthosis," *Journal of Rehabilitation Research and Development,* vol. 37, pp. 693-700, Dec. 2000.

[15] J. L. Emken, J. H. Wynne, S. J. Harkema, and D. J. Reinkensmeyer, "A robotic device for manipulating human stepping," *IEEE Transactions on Robotics,* vol. 22, pp. 185-189, Feb. 2006.

[16] E. H. F. Van Asseldonk, J. F. Veneman, R. Ekkelenkamp, J. H. Buurke, F. C. T. Van Der Helm, and H. Van Der Kooij, "The effects on kinematics and muscle activity of walking in a robotic gait trainer during zero-force control," *IEEE Transactions on Neural Systems and Rehabilitation Engineering,* vol. 16, pp. 360-370, Aug. 2008.

[17] J. v. Z. Alexander Duschau Wicke, Andrea Caprez, Lars Lunenburger, Robert Riener, "Path Control: A Method for Patient-Cooperative Robot Aided Gait Rehabilitation " *IEEE Transactions on Neural Systems And Rehabilitation Engineering,* vol. 18, pp. 38-48, Feb. 2010.

[18] J. L. Emken, R. Benitez, and D. J. Reinkensmeyer, "Human-robot cooperative movement training: Learning a novel sensory motor transformation during walking with robotic assistance-as-needed," *Journal of NeuroEngineering and Rehabilitation,* vol. 4, 2007.

[19] L. Marchal-Crespo and D. J. Reinkensmeyer, "Review of control strategies for robotic movement training after neurologic injury," *Journal of NeuroEngineering and Rehabilitation,* vol. 6, 2009.

[20] S. Hussain, "State-of-the-Art Robotic Gait Rehabilitation Orthoses: Design and Control Aspects," *NeuroRehabilitation,* vol. 35, pp. 701-709, Nov. 2014.

[21] N. Hogan, "Impedance Control: An approach to manipulation," *J. Dynamic Syst. Meas. Control,* vol. 107, pp. 1-23, 1985.

[22] S. Hussain, S. Q. Xie, and P. K. Jamwal, "Adaptive Impedance Control of a Robotic Orthosis for Gait Rehabilitation," *IEEE Transactions on Cybernetics,* vol. 43, pp. 1025-1034, Jun. 2013

[23] J. Lee, P. H. Chang, and R. S. Jamisola Jr, "Relative impedance control for dual-arm robots performing asymmetric bimanual tasks," *IEEE Trans. Ind. Electron.,* vol. 61, pp. 3786-3796, Jul. 2014.

[24] S. Jezernik, G. Colombo, and M. Morari, "Automatic gait-pattern adaptation algorithms for rehabilitation with a 4-DOF robotic orthosis," *IEEE Transactions on Robotics and Automation,* vol. 20, pp. 574-582, Jun. 2004.

[25] E. T. Wolbrecht, V. Chan, D. J. Reinkensmeyer, and J. E. Bobrow, "Optimizing compliant, model-based robotic assistance to promote neurorehabilitation," *IEEE Transactions on Neural Systems and Rehabilitation Engineering,* vol. 16, pp. 286-297, Jun. 2008.

[26] R. Riener and T. Edrich, "Identification of passive elastic joint moments in the lower extremities," *Journal of Biomechanics,* vol. 32, pp. 539-544, May. 1999.

[27] T. Edrich, R. Riener, and J. Quintern, "Analysis of passive elastic joint moments in paraplegics," *IEEE Transactions on Biomedical Engineering,* vol. 47, pp. 1058-1065, Aug. 2000.

[28] N. Hogan, H. I. Krebs, B. Rohrer, J. J. Palazzolo, L. Dipietro, S. E. Fasoli*, et al.*, "Motions or muscles? Some behavioral factors underlying robotic assistance of motor recovery," *Journal of Rehabilitation Research and Development,* vol. 43, pp. 605-618, Sep. 2006.

[29] S. K. Banala, S. K. Agrawal, S. H. Kim, and J. P. Scholz, "Novel gait adaptation and neuromotor training results using an active leg exoskeleton," *IEEE/ASME Transactions on Mechatronics,* vol. 15, pp. 216-225, Apr. 2010.

[30] A. Duschau-Wicke, A. Caprez, and R. Riener, "Patient-cooperative control increases active participation of individuals with SCI during robot-aided gait training," *Journal of NeuroEngineering and Rehabilitation,* vol. 7, 2010.

[31] S. Srivastava, P. C. Kao, S. H. Kim, P. Stegall, D. Zanotto, J. S. Higginson*, et al.*, "Assist-as-Needed Robot-Aided Gait Training Improves Walking Function in Individuals Following Stroke," *IEEE Transactions on Neural Systems and Rehabilitation Engineering,* vol. 23, pp. 956-963, Nov. 2015.

[32] D. Zanotto, P. Stegall, and S. K. Agrawal, "Adaptive assist-as-needed controller to improve gait symmetry in robot-assisted gait training," in *Proceedings - IEEE International Conference on Robotics and Automation*, 2014, pp. 724-729.

[33] W. E. I. Daisuke Aoyagi, Susan J. Harkema, David J. Reinkensmeyer, James E. Bobrow., "A Robot and Control Algorithm That Can Synchronously Assist in Naturalistic Motion

During Body-Weight-Supported Gait Training Following Neurologic Injury," *IEEE Transactions on Neural Systems And Rehabilitation Engineering,* vol. 15, pp. 387-400, Sep. 2007.
[34] D. J. Reinkensmeyer, D. Aoyagi, J. L. Emken, J. A. Galvez, W. Ichinose, G. Kerdanyan*, et al.*, "Tools for understanding and optimizing robotic gait training," *Journal of Rehabilitation Research and Development,* vol. 43, pp. 657-670, Sep. 2006.
[35] H. Yu, S. Huang, G. Chen, Y. Pan, and Z. Guo, "Human-Robot Interaction Control of Rehabilitation Robots with Series Elastic Actuators," *IEEE Transactions on Robotics,* vol. 31, pp. 1089-1100, Oct. 2015.
[36] J. F. Veneman, R. Kruidhof, E. E. G. Hekman, R. Ekkelenkamp, E. H. F. Van Asseldonk, and H. Van Der Kooij, "Design and evaluation of the LOPES exoskeleton robot for interactive gait rehabilitation," *IEEE Transactions on Neural Systems and Rehabilitation Engineering,* vol. 15, pp. 379-386, Sep. 2007.
[37] N. G. Tsagarakis and D. G. Caldwell, "Development and control of a 'soft-actuated' exoskeleton for use in physiotherapy and training," *Autonomous Robots,* vol. 15, pp. 21-33, 2003.
[38] P. Beyl, K. Knaepen, S. Duerinck, M. Van Damme, B. Vanderborght, R. Meeusen*, et al.*, "Safe and compliant guidance by a powered knee exoskeleton for robot-assisted rehabilitation of gait," *Advanced Robotics,* vol. 25, pp. 513-535, May. 2011.
[39] T. G. Sugar, J. He, E. J. Koeneman, J. B. Koeneman, R. Herman, H. Huang*, et al.*, "Design and control of RUPERT: A device for robotic upper extremity repetitive therapy," *IEEE Transactions on Neural Systems and Rehabilitation Engineering,* vol. 15, pp. 336-346, Sep. 2007.
[40] G. S. Sawicki and D. P. Ferris, "A pneumatically powered knee-ankle-foot orthosis (KAFO) with myoelectric activation and inhibition," *Journal of NeuroEngineering and Rehabilitation,* vol. 6, 2009.
[41] K. Kong, J. Bae, and M. Tomizuka, "Control of rotary series elastic actuator for ideal force-mode actuation in human-robot interaction applications," *IEEE/ASME Transactions on Mechatronics,* vol. 14, pp. 105-118, Feb. 2009.
[42] D. P. Ferris, K. E. Gordon, G. S. Sawicki, and A. Peethambaran, "An improved powered ankle-foot orthosis using proportional myoelectric control," *Gait and Posture,* vol. 23, pp. 425-428, Jun. 2006.
[43] K. E. Gordon, G. S. Sawicki, and D. P. Ferris, "Mechanical performance of artificial pneumatic muscles to power an ankle-foot orthosis," *Journal of Biomechanics,* vol. 39, pp. 1832-1841, Jul. 2006.
[44] C. R. Kinnaird and D. P. Ferris, "Medial gastrocnemius myoelectric control of a robotic ankle exoskeleton," *IEEE Transactions on Neural Systems and Rehabilitation Engineering,* vol. 17, pp. 31-37, Feb. 2009.
[45] D. G. Caldwell, N. G. Tsagarakis, S. Kousidou, N. Costa, and I. Sarakoglou, ""Soft" exoskeletons for upper and lower body rehabilitation - Design, control and testing," *International Journal of Humanoid Robotics,* vol. 4, pp. 549-573, 2007.
[46] N. Costa and D. G. Caldwell, "Control of a biomimetic "soft-actuated" 10DoF lower body exoskeleton," in *Proceedings of the First IEEE/RAS-EMBS International Conference on Biomedical Robotics and Biomechatronics, 2006, BioRob 2006*, 2006, pp. 495-501.
[47] C. Wang, Y. Fang, S. Guo, and Y. Chen, "Design and kinematical performance analysis of a 3-RUS/RRR redundantly actuated parallel mechanism for ankle rehabilitation," *Journal of Mechanisms and Robotics,* vol. 5, Jul. 2013.
[48] S. Hussain, S. Q. Xie, P. K. Jamwal, and J. Parsons, "An Intrinsically Compliant Robotic Orthosis for Treadmill Training.," *Medical Engineering and Physics,* vol. 34, pp. 1448-1453, Dec. 2012
[49] A. Zelinsky, "Robot suit hybrid assistive limb," *IEEE Robotics and Automation Magazine,* vol. 16, 2009.
[50] E. T. Wolbrecht, D. J. Reinkensmeyer, and J. E. Bobrow, "Pneumatic control of robots for rehabilitation," *International Journal of Robotics Research,* vol. 29, pp. 23-38, May. 2010.
[51] S. Hussain, S. Q. Xie, and P. K. Jamwal, "Robust Nonlinear Control of an Intrinsically Compliant Robotic Gait Training Orthosis. ," *IEEE Transactions on Systems, Man, and Cybernetics: Systems,* vol. 43, pp. 655-665, May. 2013
[52] S. Hussain, S. Q. Xie, and P. K. Jamwal, "Control of a Robotic Orhtosis for Gait Rehabilitation," *Robotics and Autonomous Systems,* vol. 61, pp. 911-919, Sep. 2013.
[53] D. B. Reynolds, D. W. Repperger, C. A. Phillips, and G. Bandry, "Modeling the dynamic characteristics of pneumatic muscle," *Annals of Biomedical Engineering,* vol. 31, pp. 310-317, 2003.
[54] J.-J. E. Slotine and W. Li, *Applied NonLinear Control*. NJ: Prentice-Hall, Inc 1991.
[55] D. A. Winter, *The Biomechanics and Motor Control of Human Gait: Normal, Elderly and Pathological*, 2nd ed. Waterloo: University of Waterloo Press, 1991.
[56] J. M. Hidler and A. E. Wall, "Alterations in muscle activation patterns during robotic-assisted walking," *Clinical Biomechanics,* vol. 20, pp. 184-193, Feb. 2005.
[57] F. Wilcoxon, "Individual comparisons of grouped data by ranking methods," *Journal of economic entomology,* vol. 39, p. 269, Apr. 1946.

Shahid Hussain received the M.E. and Ph.D. degrees in mechanical engineering from The University of Auckland, Auckland, New Zealand, in 2009 and 2013, respectively. He is a lecturer at University of Wollongong, Australia. His research interests include robot-assisted rehabilitation, compliant actuation of robots, human–robot interaction, biomechanical modelling of musculoskeletal system and nonlinear control of dynamic systems.

Prashant K. Jamwal (M'15) earned his Ph.D. from the University of Auckland, Auckland, New Zealand and obtained Master of Technology from I.I.T., Roorkee, India. He is a faculty member at Nazarbayev University, Astana. His research interests include artificial intelligence, fuzzy mathematics and its applications, smart sensors and actuators, bio-mechatronics, biomedical robotics, evolutionary algorithms and multi-objective optimization. He has more than 20 years of teaching and research experience.

Mergen H. Ghayesh received the Ph.D degree in Mechanical Engineering from the Department of Mechanical Engineering, McGill University, Montreal, Canada, in 2013. He currently serves as an Assistant Professor at University of Adelaide, Australia. His research interests include dynamics, vibration, and control of macro/micro/nano systems. He has published more than 100 refereed journal papers in his areas of research.

Sheng (S. Q.) Xie (SM'11) received his Ph.D. degree in Manufacturing Automation from the University of Canterbury, Canterbury, New Zealand in 2002. He is currently a Chair Professor in the area of (Bio-) mechatronics at the University of Auckland, New Zealand. His current research interests are smart sensors and actuators, medical and rehabilitation robots, MEMS, modern control technologies and applications, and rapid product development technologies, methods, and tools. Prof. Xie is the technical editor for *IEEE/ASME Transactions on Mechatronics*.